Cellular/Molecular

Loss of Adult 5-HT1A Autoreceptors Results in a Paradoxical Anxiogenic Response to Antidepressant Treatment

Valérie Turcotte-Cardin,[1,2] Faranak Vahid-Ansari,[1,2] Christine Luckhart,[1,2] Mireille Daigle,[1] Sean D. Geddes,[2] Kenji F. Tanaka,[3] René Hen,[4] Jonathan James,[5] Zul Merali,[5] Jean-Claude Béïque,[2] and Paul R. Albert[1,2]

[1]Ottawa Hospital Research Institute (Neuroscience), University of Ottawa, Ottawa, Ontario K1H 8M5, Canada, [2]Department of Cellular and Molecular Medicine, University of Ottawa Brain and Mind Research Institute, Ottawa, Ontario K1H 8M5, Canada, [3]Department of Neuropsychiatry, School of Medicine, Keio University, Tokyo, 160-8582, Japan, [4]New York State Psychiatric Institute and Department of Psychiatry, Columbia University, New York, New York 10032, and [5]Royal's Institute of Mental Health, University of Ottawa, Ottawa, Ontario, K1Z 7K4 Canada

Selective serotonin (5-HT) reuptake inhibitors (SSRIs) are first-line antidepressants but require several weeks to elicit their actions. Chronic SSRI treatment induces desensitization of 5-HT1A autoreceptors to enhance 5-HT neurotransmission. Mice (both sexes) with gene deletion of 5-HT1A autoreceptors in adult 5-HT neurons (*1AcKO*) were tested for response to SSRIs. Tamoxifen-induced recombination in adult *1AcKO* mice specifically reduced 5-HT1A autoreceptor levels. The *1AcKO* mice showed a loss of 5-HT1A autoreceptor-mediated hypothermia and electrophysiological responses, but no changes in anxiety- or depression-like behavior. Subchronic fluoxetine (FLX) treatment induced an unexpected anxiogenic effect in *1AcKO* mice in the novelty suppressed feeding and elevated plus maze tests, as did escitalopram in the novelty suppressed feeding test. No effect was seen in wild-type (*WT*) mice. Subchronic FLX increased 5-HT metabolism in prefrontal cortex, hippocampus, and raphe of *1AcKO* but not *WT* mice, suggesting hyperactivation of 5-HT release. To detect chronic cellular activation, FosB $^{+}$ cells were quantified. FosB $^{+}$ cells were reduced in entorhinal cortex and hippocampus (CA2/3) and increased in dorsal raphe 5-HT cells of *1AcKO* mice, suggesting increased raphe activation. In *WT* but not *1AcKO* mice, FLX reduced FosB $^{+}$ cells in the median raphe, hippocampus, entorhinal cortex, and median septum, which receive rich 5-HT projections. Thus, in the absence of 5-HT1A autoreceptors, SSRIs induce a paradoxical anxiogenic response. This may involve imbalance in activation of dorsal and median raphe to regulate septohippocampal or fimbria-fornix pathways. These results suggest that markedly reduced 5-HT1A autoreceptors may provide a marker for aberrant response to SSRI treatment.

Key words: 5-HT1A receptor; anxiety; autoreceptor; knock-out; raphe; serotonin

Significance Statement

Serotonin-selective reuptake inhibitors (SSRIs) are effective in treating anxiety and depression in humans and mouse models. However, in some cases, SSRIs can increase anxiety, but the mechanisms involved are unclear. Here we show that, rather than enhancing SSRI benefits, adulthood knockout (KO) of the 5-HT1A autoreceptor, a critical negative regulator of 5-HT activity, results in an SSRI-induced anxiety effect that appears to involve a hyperactivation of the 5-HT system in certain brain areas. Thus, subjects with very low levels of 5-HT1A autoreceptors, such as during childhood or adolescence, may be at risk for an SSRI-induced anxiety response.

Introduction

Major depression is a prevalent and multifactorial mental illness involving genetic and environmental stressors that negatively affect mood and emotion (Krishnan and Nestler, 2008; aan het Rot et al., 2009; Northoff, 2013). Depressive symptoms are correlated with reduced 5-HT neurotransmission and can be precipitated in recovered depressed subject by acute tryptophan depletion, which lowers 5-HT levels (Young and Leyton, 2002; Jans et al.,

Received Feb. 6, 2018; revised Dec. 6, 2018; accepted Dec. 7, 2018.

Author contributions: V.T.-C., F.V.-A., and P.R.A. wrote the first draft of the paper; V.T.-C., F.V.-A., C.L., M.D., S.D.G., K.F.T., R.H., J.J., Z.M., J.-C.B., and P.R.A. edited the paper; V.T.-C., F.V.-A., C.L., S.D.G., and P.R.A. designed research; V.T.-C., F.V.-A., C.L., M.D., S.D.G., and J.J. performed research; K.F.T. and R.H. contributed unpublished reagents/analytic tools; V.T.-C., F.V.-A., C.L., M.D., S.D.G., J.J., Z.M., J.-C.B., and P.R.A. analyzed data; P.R.A. wrote the paper.

This work was supported by Canadian Institutes for Health Research Grants MOP-115098 and MOP-123426 to P.R.A., and Canadian Partnership for Stroke Recovery trainee support to F.V.-A. These agencies had no role in the design of the study, collection, and analysis of data or decision to publish. We thank Dr. Diane Lagace and the University of Ottawa Behavioral Core for helpful advice and technical assistance.

The authors declare no competing financial interests.

Correspondence should be addressed to Paul R. Albert at palbert@uottawa.ca.

https://doi.org/10.1523/JNEUROSCI.0352-18.2018

 0270-6474/19/391334-13$15.00/0

2007). The 5-HT1A receptor is widely expressed in the brain to regulate mood and emotion, both as a postsynaptic heteroreceptor, and as a major presynaptic autoreceptor in 5-HT neurons of the raphe nuclei. The 5-HT1A receptor is an inhibitory Gi/Go-coupled receptor (Albert et al., 1996) that negatively regulates 5-HT neuronal firing activity via negative feedback upon release of 5-HT (Albert, 2012; Blier and El Mansari, 2013). An increase in raphe 5-HT1A autoreceptor level is observed in depressed subjects by PET imaging using the 5-HT1A antagonist [^{11}C]-WAY100635 (Hesselgrave and Parsey, 2013). Similarly, a specific increase in 5-HT1A binding in the rostral dorsal raphe was seen by autoradiography studies of postmortem brains of depressed suicide victims, using the 5-HT1A-selective agonist [^{3}H]-DPAT (Stockmeier et al., 1998; Boldrini et al., 2008). Thus, an elevated level of 5-HT1A autoreceptors and reduced 5-HT neurotransmission are associated with human depression, and in mouse depression models (Albert et al., 2014; Garcia-Garcia et al., 2014).

Selective serotonin reuptake inhibitors (SSRIs) are first-line antidepressants due to their specificity and tolerability (Cipriani et al., 2009; Rush et al., 2009). However, antidepressant treatments have a delay of several weeks before an appreciable antidepressant effect is seen, and this can lead to patients discontinuing prescription use and increased suicide attempts. Increased levels of 5-HT1A autoreceptors could account for the delay in SSRI action (Albert, 2012; Coplan et al., 2014). Acute SSRI treatment induces a transient increase in 5-HT in target areas and in the raphe. Negative feedback from raphe 5-HT1A autoreceptors reduces 5-HT neuronal firing. Following chronic SSRI treatment, 5-HT1A autoreceptors desensitize, leading to disinhibition of 5-HT neurons to enhance their firing rate and increase in 5-HT release (Piñeyro and Blier, 1999; Albert and Lemonde, 2004). Accordingly, mice with a partial suppression of raphe 5-HT1A autoreceptor levels displayed resilience to chronic stress and a robust and rapid (within 8 d) response to chronic SSRI fluoxetine (FLX), whereas *WT* mice showed no response even after 26 d of treatment (Richardson-Jones et al., 2010). Similarly, using siRNA to reduce the expression of 5-HT1A autoreceptors acutely during adulthood has an antidepressant-like effect and does not affect the anxiety levels in rats (Bortolozzi et al., 2012). Conversely, upregulation of 5-HT1A autoreceptors by 5-HT neuron-specific KO of the *HTR1A gene* repressor Freud-1 results in FLX-resistant anxiety and depression in mice (Vahid-Ansari et al., 2017). These results suggest that SSRI action is enhanced when 5-HT1A autoreceptors are partially depleted but is attenuated when they are upregulated.

Based on the findings above, we generated an inducible conditional *HTR1A* KO mouse (*1AcKO*) to excise the 5-HT1A gene specifically in 5-HT neurons during adulthood. We find that the *1AcKO* mice had no significant change in baseline anxiety- or depression-like behaviors. Upon subchronic treatment with SSRIs, however, we observed an unexpected anxiogenic effect. In *1AcKO* mice, we found increased FLX-induced 5-HT metabolism, consistent with a hyperactive 5-HT system. We also found FLX-induced changes in FosB$^+$ cells specific to *1AcKO* in raphe, hippocampal, and entorhinal cortex (EC). These findings may provide a model for the proanxiety effects of a hyperactivated 5-HT system on response to SSRI treatment.

Materials and Methods

Animals. TPH2-Cre^{ERT2} mice (stock #016584, C57BL/6N background, The Jackson Laboratory, https://www.jax.org/strain/016584; RRID: IMSR_JAX:016584) were bred to *flx-5HT1A* mice (Samuels et al., 2015) to create an inducible, conditional 5-HT1A KO (designated *1AcKO* mice). To maintain the mouse line, heterozygous mice for the *flx-5-HT1A* gene and hemizygous for the TPH2-Cre^{ERT2} gene were mated to obtain *TPH2-Cre^{ERT2}/5-HT1A-WT* and *1AcKO* littermates. Mice were single-housed in standard Plexiglas cages on a 12 h light/dark cycle with *ad libitum* access to food and water. All animal studies and experimental procedures were approved by the University of Ottawa Animal Care Committee in accordance with guidelines established by the Canadian Council of Animal Care.

TPH2-Cre^{ERT2}-flx5HT1A genotype. DNA was extracted (REDExtract-N-AMP Tissue PCR kit, Sigma-Aldrich) from tissue samples and amplified using two sets of PCR primers. The primers (2 μM) for the *flx-5HT1A* gene were as follows: 1A-5, 5′-GGG CGT CCT CTT CAC GTA G-3′ and 1A-7, 5′-CAG GGA CGT TGT GGT GTT GT-3′, and PCR was done using ONE-Taq Mastermix (New England Biolabs) yielding 254 bp (*WT*) or 292 bp (*flx-5HT1A*) products. The PCR cycle was as follows: 94°C, 2 min; 15 cycles, 94°C, 30 s; 68°C, 30 s/−0.5°C cycle; 68°C, 20 s; 20 cycles, 94°C, 30 s; 68°C, 30 s; 68°C for 20 s; 68°C for 5 min. The primers (2 μM) for *TPH2-Cre^{ERT2}* were as follows: 5′-GCT GAG AAA GAA AAT TAC ATC G-3′, 5′-TGG CTT GCA GGT ACA GGA GG-3′, 5′-CAA ATG TTG CTT GTC TGG TG-3′, and 5′-GCT AGT CGA GTG CAC AGT TT-3′, and PCR was done using EasyTaq buffer and polymerase (Transgen Biotech), yielding a 200 bp product. The PCR cycle was as follows: 94°C, 1 min; 35 cycles, 94°C, 15 s, 57°C, 20 s, 72°C, 10 s; 72°C, 2 min. Each mouse was genotyped both at weaning and at death.

Drugs and treatment. Tamoxifen (catalog #T5648) and escitalopram (ESC, catalog #E4786Z) were obtained from Sigma-Aldrich, and FLX was obtained from Enzo Biosciences (catalog #BML-NS140-0250). Both ESC (30 mg/kg/d) and FLX (18 mg/kg/d) were dissolved in water and administered in the drinking water (vehicle). Drug consumed was determined by measuring the amount of drinking water consumed every 3 d (~3 ml/d) and did not differ between groups. To accurately measure treatment consumption, for behavioral assays mice were single housed at the start of treatment until perfusion. The dose for both drugs was chosen based on previous studies showing that they are clinically relevant doses (Santarelli et al., 2003; Berger et al., 2012). Tamoxifen (180 mg/kg, i.p.) was dissolved in ethanol, diluted in sunflower oil (30% ethanol), and administered to both *WT* and *1AcKO* mice on three consecutive days.

Immunofluorescence. Mice were anesthetized (Euthanyl; 0.01 ml/g), perfused by cardiac infusion of PBS followed by 4% PFA via the left ventricle. Whole brains were extracted, postfixed in 4% PFA for 1 h. Brains were kept in 30% sucrose solution, changed daily for 4 d and frozen. Coronal brain slices (n = 8 slices, 25 μm) were taken using a cryostat with respect to bregma to match sections across groups. Bregma values (millimeters) and templates (micrometers) for cell counting were as follows: EC (−1.94; 210 × 305), NAc (0.98, 321 × 428), medial (MSN, 0.26, 85 × 210), and lateral septum (LSN, 0.26, 80 × 100), rostral hippocampus (−1.22), CA1 (138 × 210), CA2/3 (321 × 428), DG (321 × 428), amygdala (Amy, −1.94, 80 × 128), lateral habenula (LHb, −1.94, 80 × 100), and raphe nuclei (DR, bregma −4.16, −4.41, −4.66, −4.91, comprising four 25 μm slices/brain), median (MR, 150 × 875), and dorsal raphe (DR, 321 × 650). Slices were thaw-mounted on Superfrost slides (Thermo Fisher Scientific) and stored at −80°C. Staining was done using antibodies to YFP (1:500 chicken anti-GFP, Abcam ab13970, RRID:AB_300798; secondary, 1:250 CY3-goat anti-chicken, Jackson ImmunoResearch Labortories 103–545-155, RRID:AB_2337390); TPH (1:100 sheep anti-TPH, Millipore ab1541, RRID:AB_90754; secondary, 1:200 CY2-donkey anti-sheep, Jackson ImmunoResearch Labortories 713-165-003; RRID:AB_2340727); 5-HT1A receptor (purified anti-5-HT1A 1:50) (Czesak et al., 2012), secondary, AlexaFluor-donkey anti-rabbit (1:1000, Thermo Fisher Scientific, A-21206, RRID:AB_2535792); or FosB (1:500 rabbit anti-FosB, Santa Cruz Biotechnology sc-48, RRID: AB_631515; secondary, 1:1000 AlexaFluor-donkey anti-rabbit), with conditions as previously described (Vahid-Ansari et al., 2017; Vahid-Ansari and Albert, 2018). Images were acquired on an Axio Observer D1 microscope (Carl Zeiss, <20× magnification) and analyzed using Axiovision imaging software (RRID:SCR_002677). Positively stained cells co-localized with DAPI were manually counted in a blinded procedure, within standardized templates (see Results) drawn by ImageJ 1.48 version software (RRID:SCR_003070). Cell counts for quantification of

FosB$^+$ cells were done as described previously (Vialou et al., 2015; Vahid-Ansari and Albert, 2018) using 1 field/brain region, 1 section/area except raphe (4 sections), with the number and sex of animals shown as data points in figures.

5-HT1A receptor autoradiography. *WT* and *1AcKO* littermate mice (14 weeks old, $n = 3$/group) were killed by cervical dislocation and decapitation. Extracted brains were immediately frozen on dry ice and stored at −80°C until sectioning. Brains were cryosectioned (25 μm), mounted on Superfrost Slides, and maintained at −80°C until processing. Sections were processed for [^{125}I]MPPI (PerkinElmer) autoradiography as described previously (Vahid-Ansari et al., 2017), and exposed to Kodak BioMax MR film (VWR) for 7 h. Films were scanned at 1200 dpi resolution using an Epson Perfection V500 Photo Scanner. Signal density was quantified using the mean luminosity function in ImageJ. The level of 5-HT1A binding (μCi) was quantified by standardizing the signal density to an adjacent background with nonspecific binding. Sections between bregma −4.36 mm and −4.60 mm were averaged for the DR and MR, and bregma −1.82 mm was used for the hippocampus. Signals fell within the linear range of the film and were quantified following the standard curve using ARC146-F ^{14}C standard (American Radiochemicals).

Whole-cell electrophysiology. Brainstem slices (300 μm) were prepared from 12- to 15-week-old mice as previously described (Geddes et al., 2016). Slices were incubated in a chamber bubbled with 95% O_2 and 5% CO_2 and containing standard Ringer's solution. DR neurons were visualized using an upright microscope equipped with differential interference contrast optics (Olympus BX51W1; 40×/0.80 NA objective), and 5-HT cells were identified using morphological and biophysical characteristics previously established (Calizo et al., 2011; Geddes et al., 2016). Whole-cell recordings were acquired using an Axon Multiclamp 700B amplifier and digitized with an Axon Digidata 1440A (or 1550) digitizer. The borosilicate glass electrodes were filled with an internal solution containing 115 mM potassium gluconate, 20 mM KCl, 10 mM sodium phosphocreatine, 10 mM HEPES, 4 mM ATP(Mg^{2+}), and 0.5 mM GTP, pH 7.25 (adjusted with KOH; osmolarity, 280–290 mOsmol/L). To determine the function of 5-HT1A autoreceptor, we monitored the effects of the nonselective 5-HT1A agonist 5-CT (100 nM). For all voltage-clamp recordings, access resistance was continuously monitored by applying a 125 ms, 2 mV hyperpolarizing pulse every 10 s. Recordings were discarded if the access resistance changed by >30% during the course of the recordings.

HPLC analysis. Levels of 5-HT and 5-hydroxy indole acetic acid (5-HIAA) were quantified in extracts of dissected tissues by HPLC (Vahid-Ansari et al., 2017). For HPLC, mice were killed by cervical dislocation and decapitation, and dorsal raphe, hippocampus, and PFC were dissected, pooled, frozen immediately on dry ice, and maintained at −80°C until homogenization. In brief, 300 μl of homogenization solution (0.3 M monochloroacetic acid, 0.1 mM EDTA, 10% methanol and internal standard) was added to each sample followed by sonication. Following sonication, 100 μl was aliquoted and frozen for protein concentration determination (Pierce Coomassie Bradford Protein Assay). The remaining 200 μl was centrifuged and the supernatant analyzed for 5-HT and 5-HIAA content using HPLC (Agilent Technologies). A 10 μl volume of supernatant was injected into the HPLC system reverse-phase analytical column (Phenomenex Kinetex 2.6 μm C-18, 100 × 4.6 mm) and electrochemical detector (VT-03 flow cell, Intro detector; Antec Leyden), with an applied potential of 500 mV, a filter of 1 s, and a range of 100 nA/V. The flow rate was 0.5 ml/min with mobile phase consisting of (in mM) as follows: 90 NaH_2PO_4, 1.7 1-octane sulfonic acid (sodium salt), 50 citric acid (monohydrate), 5 KCl, 50 EDTA, and 14% acetonitrile, final pH 3.0. Quantification of analytes was performed by comparing area under the curve with known external standards using computerized ChemStation chromatography data acquisition system (Agilent Technologies).

8OH-DPAT-induced hypothermia. The hypothermia procedure was performed between 11:00 A.M. and 4:00 P.M. Mice were weighed, and internal temperature was taken using a rectal thermometer every 10 min for 40 min (4 baseline measurements). Animals were administered 8OH-DPAT (0.75 mg/kg, i.p., Sigma-Aldrich) or vehicle (0.9% saline) followed by six measurements of post-treatment body temperature at 10 min intervals. Each mouse received saline injection on the first day and 8OH-DPAT injection on the third day. For analysis purposes, the first baseline temperature was discarded. The remaining three baseline values were averaged, and the difference between the average baseline and recorded temperature was plotted across time.

Behavioral testing. All behavior tests were performed in the University of Ottawa Behavioral Core Facility using 11-week-old *1AcKO* and *WT* littermate mice between 9:00 A.M. and 4:00 P.M. One test was done per day, and experimental apparati were cleaned between each trial (Vahid-Ansari et al., 2017). The behavioral phenotype of *1AcKO* versus *WT* mice was investigated in several cohorts by 2 different experimenters who were blind to each mouse condition (genotype and treatment). At the start of treatment, mice were single housed and maintained on treatment until perfusion. In each cohort, the proportion of males/females was close to equal, plotted as blue and pink symbols, respectively. For females, estrous cycle staining was done at the end of behavioral testing. Vaginal smears were taken from 20 female *WT* and *1AcKO* mice every day at 2:00 P.M. for 4 consecutive days, the length of the mouse estrous cycle. Smears were dried overnight on Superfrost slides (Thermo Fisher Scientific) and stained with 0.1% cresyl violet (Sigma-Aldrich) and staged (McLean et al., 2012). Estrus cycle staging revealed a relatively similar distribution of each cycle (proestrus, estrus, metestrus/diestrus) between each genotype across the 4 d of testing, as reported in normal mice (McLean et al., 2012). Mice were kept under their respective antidepressant treatment during all the tests until they were killed.

Novelty suppressed feeding (NSF) test. Mice were food restricted for 24 h and placed in a corner of a 45 × 45 × 45 cm open box with bedding, overhead illumination (100 lux), and a pellet in the center. Latency for the mouse to first approach to the food within 10 min was recorded. Mice were returned to the home cage with a weighed food pellet, and the latency to feed and total food consumption after 5 min was recorded.

Light dark box (LD). Each mouse was placed in a soundproof square chamber equally divided into two chambers measuring 27 × 13.5 cm for 10 min (Vahid-Ansari et al., 2016). The dark compartment was covered in black plastic, and the light compartment is transparent, uncovered, and lit with two bulbs at 390 lux (Med Associates) with an opening allowing movement between chambers. Movement was detected by infrared transmitters and receivers placed around the chamber periphery.

Elevated plus maze (EPM). The mouse was placed in the center of an elevated track with two 6-cm-wide and 75-cm-long arms crossed in the center at a perpendicular angle (Noldus) for 10 min. The closed arm was enclosed by walls 20 cm tall, whereas the open arm had no walls. An overhead illumination (100 lux) and a camera linked to the Ethovision tracking program (Ethovision 11.5, Noldus Information Technologies) recorded mouse movement.

Tail suspension (TS). Each mouse's tail was taped horizontally on an aluminum bar attached to a transducer detecting the force of movement for 6 min. Immobility time was quantified as movement below a set threshold (Med Associates).

Forced swim test (FST). Each mouse was placed in a clear Plexiglas cylinder filled with 23°C–25°C tap water up to 5–10 cm from the top for 6 min under red light. A camera placed in front of the cylinder recorded the movement, and the immobility time was quantified using Ethovision software (Noldus).

Statistical analysis. All statistical analyses and graphs were done using Prism version 6 (GraphPad Software, RRID:SCR_002798). Data are shown as mean ± SEM. For behavioral and immunofluorescence studies, outliers were identified using the ROUT method in Prism 6 (GraphPad Software) and were excluded from the analysis. Data comparing the *WT* versus *1AcKO* mice on one outcome measure were analyzed using an unpaired *t* test with $p < 0.05$ considered significant. For data comparing across genotype and treatment, two-way ANOVA was used and all *post hoc* comparisons were made with Tukey's multiple-comparisons test.

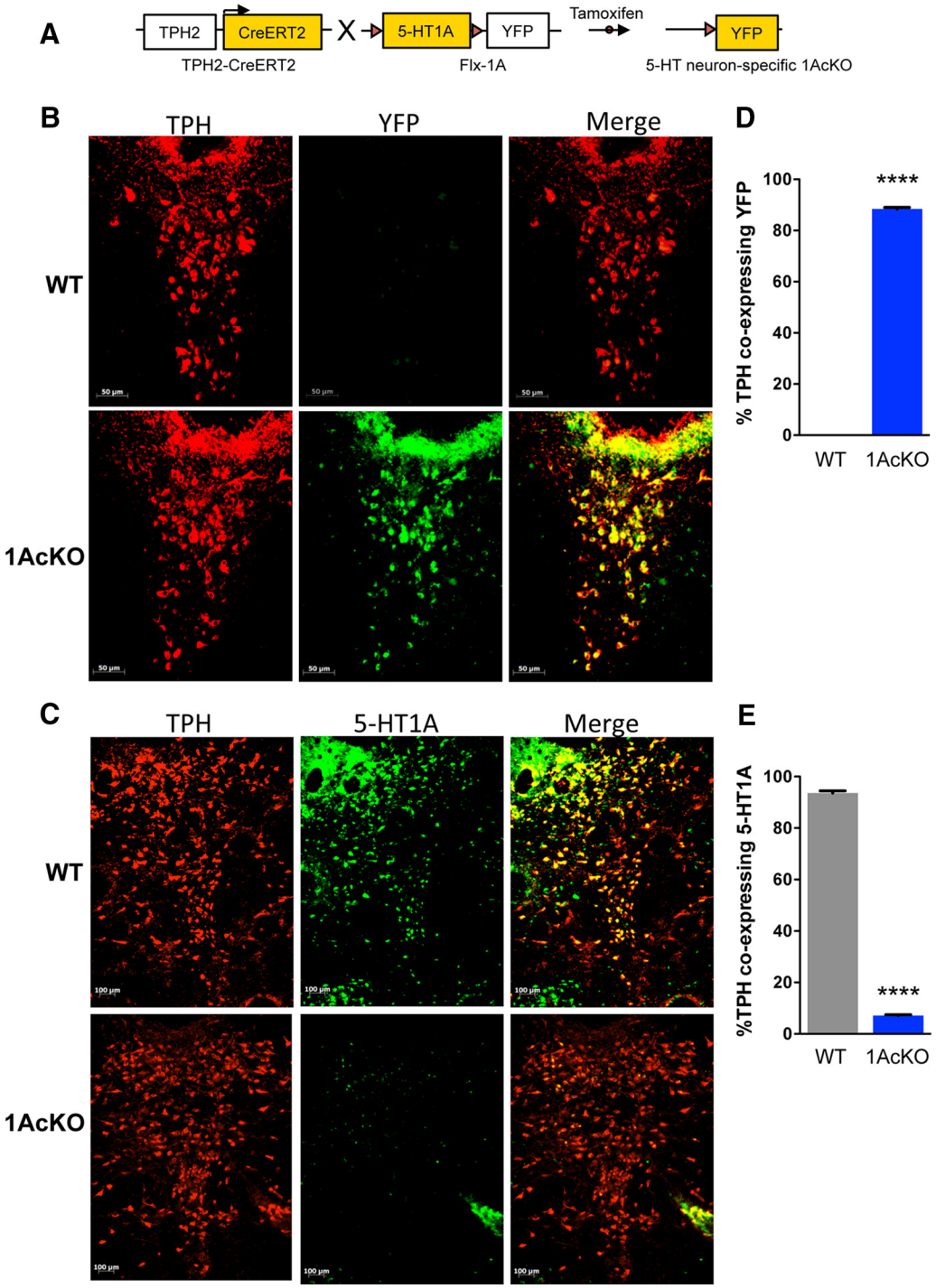

Figure 1. Loss of 5-HT1A autoreceptors in adult 5-HT neurons of *1AcKO* mice. ***A***, Conditional KO strategy. To KO the *HTR1A* gene in adult 5-HT neurons, *TPH2-CreERT2* and *flx-5HT1A* mice were bred to generate *1AcKO* mice; upon treatment with tamoxifen, the 5-HT1A gene is knocked out and yellow fluorescent protein (YFP) is expressed in TPH$^+$ serotonin neurons. ***B***, ***C***, Tamoxifen-induced YFP expression and 5-HT1A receptor loss in dorsal raphe (DR) 5-HT neurons. DR sections from tamoxifen-treated *1AcKO* and *WT* littermates were stained for TPH (5-HT neuron marker) and YFP (marker of recombination) or 5-HT1A receptor. Scale bar is shown. ***D***, ***E***, Quantification of TPH/YFP- and TPH/5-HT1A-positive cells. Data are mean ± SE ($n = 4$), ****$p < 0.0001$ (unpaired two-tailed Student's *t* test). ***D***, $t = 152.9$ df $= 6$; E, $t = 90.39$ df $= 4$. No YFP signal was detected in other brain regions (see Figure 1-1, available at https://doi.org/10.1523/JNEUROSCI.0352-18.2018.f1-1).

Results

Specific loss of 5-HT1A autoreceptor protein and function in *1AcKO* mice

To address the role of 5-HT1A autoreceptors in adulthood, we generated mice with conditional, inducible KO of the *HTR1A* gene by mating *TPH2-Cre^{ERT2}* and *flx-5HT1A* mice to generate the *1AcKO* mice (Fig. 1*A*). Because the *flx-5HT1A* mice have a yellow fluorescent protein (YFP) cassette inserted downstream of the 5-HT1A coding sequence that is induced upon recombination, YFP can be used as a marker of recombination. In adult *1AcKO* but not *WT* littermates treated from postnatal days 53–55 with tamoxifen to induce recombination, 2 weeks later YFP expression was seen in TPH$^+$ (5-HT) cells of the dorsal raphe nucleus (Fig. 1*B*,*D*), but not in nonserotonergic brain regions, such

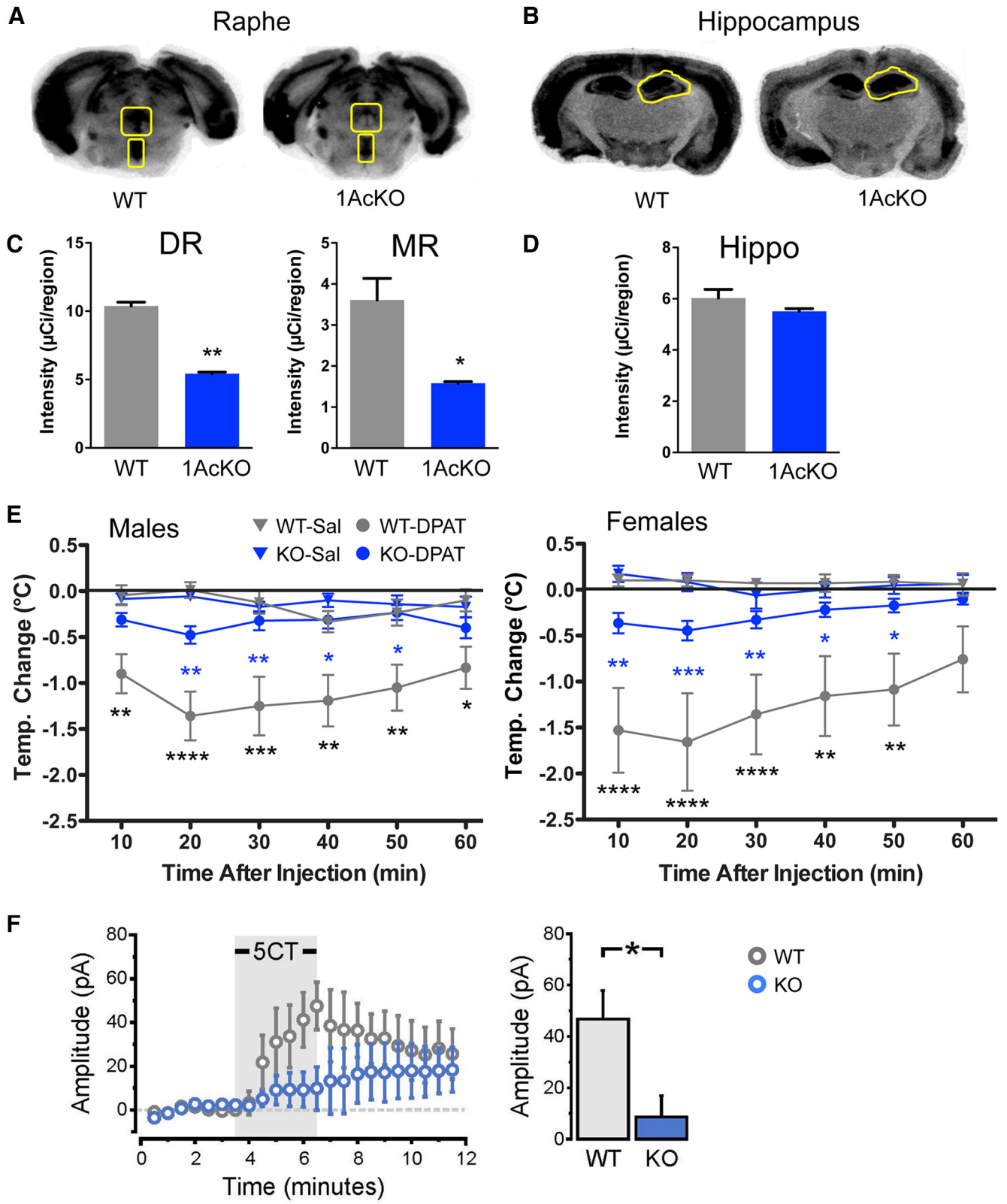

Figure 2. Loss of raphe 5-HT1A binding and autoreceptor function in *1AcKO* mice. ***A***, ***B***, 5-HT1A receptor autoradiography of raphe and hippocampus. Top, Representative images of [^{125}I]MPPI autoradiography of sections from *1AcKO* and *WT* littermate mice showing dorsal (DR) and median (MR) raphe (***A***; boxes) and hippocampal (***B***; circumscribed) regions. ***C***, ***D***, Average intensity (μCi/region) was quantified for each region using templates above. Data are mean ± SEM (n = 3/group), unpaired two-tailed Student's t test. DR: $^{**}p = 0.0039$, $t = 16.05$ df = 3; MR: $^{*}p = 0.0147$, $t = 5.088$ df = 3; hippocampus: $p = 0.1999$, not significant, $t = 1.440$ df = 6. ***E***, 5-HT1A-induced hypothermia. In *WT*, 8OH-DPAT (DPAT: 0.75 mg/kg, i.p.) induced body temperature reduction compared with saline (Sal), which was abolished in *1AcKO* mice in both males and females. Data are mean ± SE (n = 7–12/group). Two-way ANOVA, Tukey's post-test showed significant changes for the following: *WT*-DPAT versus *WT*-Sal (black stars, below DPAT data); and *WT*-DPAT versus *1AcKO*-DPAT (blue stars, between DPAT data); $^{*}p < 0.05$; $^{**}p < 0.01$; $^{***}p < 0.001$; $^{****}p < 0.0001$ (for statistics, see Figure 2-1, available at https://doi.org/10.1523/JNEUROSCI.0352-18.2018.f2-1; and Figure 2-2, available at https://doi.org/10.1523/JNEUROSCI.0352-18.2018.f2-2). The pretreatment temperatures (°C) were as follows (mean ± SD): M-SalWT, 38.0 ± 0.24; KO, 38.0 ± 0.24; M-DPAT WT, 38.6 ± 0.50; KO, 38.3 ± 0.31; (*Figure legend continues.*)

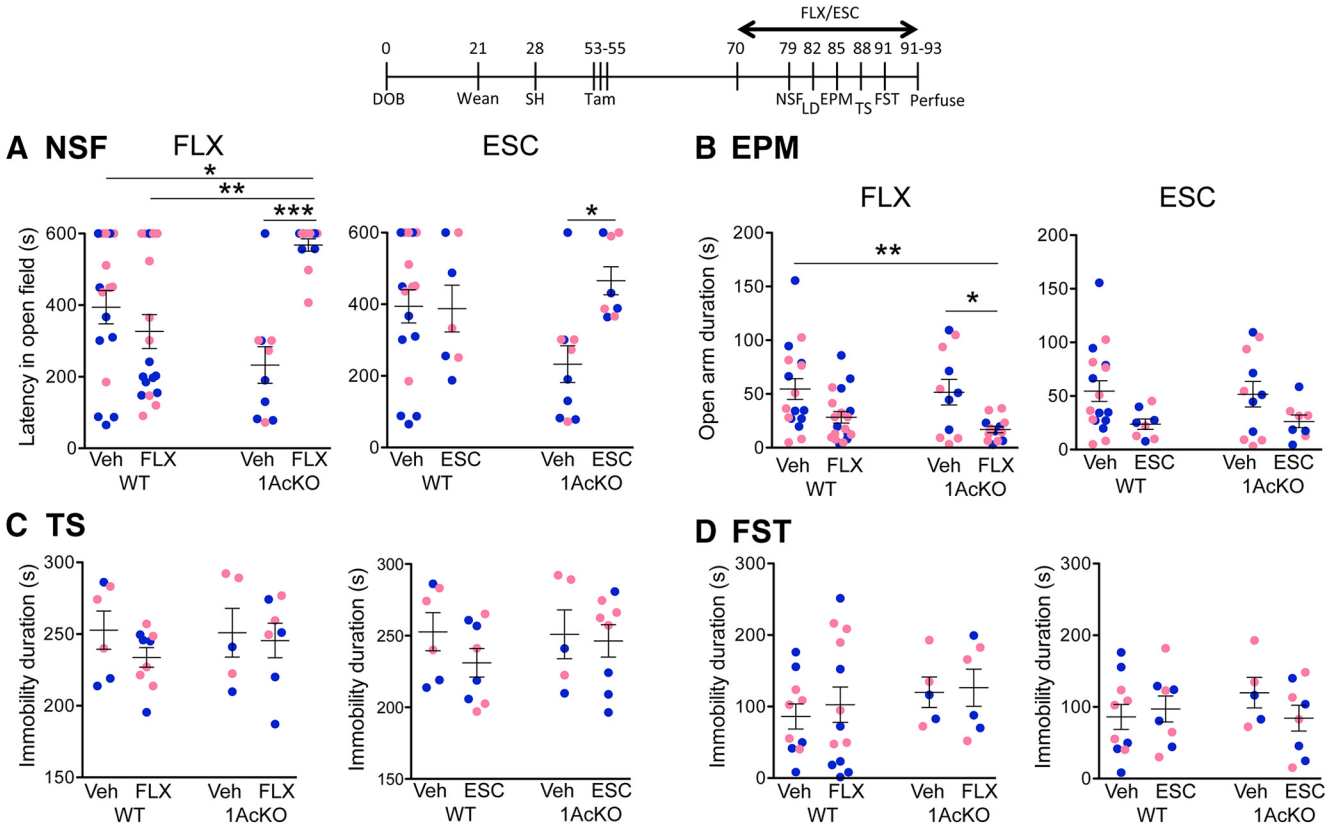

Figure 3. Anxiogenic response to subchronic selective serotonin reuptake inhibitor (SSRI) treatment in *1AcKO* mice. Top, Experimental timeline. At the start of antidepressant treatment, *WT* and *1AcKO* mice were single-housed (SH), treated with tamoxifen (Tam), and treated with fluoxetine (FLX), escitalopram (ESC), or vehicle (Veh). After 9 d, the mice tested using the indicated behavior tests, maintaining treatment, and sacrificed at the end testing. Data points from individual male (M, blue) and female (F, pink) mice are shown. ***A***, SSRI-induced anxiety in *1AcKO* in the novelty suppressed feeding (NSF) test. Vehicle, FLX, and ESC were administered to WT (*n* (M/F (outlier)) = 9/8 (2), 8/11, 4/4, respectively) and *1AcKO* (*n* = 6/4 (1), 5/7, 4/4, respectively) mice. Latency to feed in novel cage was recorded. FLX versus Veh: $F_{(3,53)} = 7.941$, $p = 0.0002$; ESC versus Veh, $F_{(3,38)} = 3.172$, $p = 0.0351$. ***B***, FLX-induced anxiety in *1AcKO* mice in the elevated plus maze (EPM) test. Vehicle, FLX, and ESC were administered to WT (*n* = 9/8, 8/11, 4/4, respectively) and KO (*n* = 6/6, 5/8 (1), 4/4, respectively), and time spent in the open arm was measured. FLX versus VEH: $F_{(3,56)} = 4.128$, $p = 0.0103$; ESC versus VEH: $F_{(3,40)} = 1.938$, $p = 0.1389$. ***C***, ***D***, Tail suspension (TS) and forced swim test (FST). For TS: WT, *n* (M/F (outlier)) = 3/3, 4/5, 4/4; KO, *n* = 2/3, 4/3, 4/4; for FST: WT *n* = 5/5, 7/6, 4/4; KO, *n* = 2/3 (1), 3/3, 4/4, for Veh, FLX, ESC, respectively. No effect of FLX or ESC was seen on immobility time in these two tests of depression-like behavior. TS versus VEH: FLX, $F_{(3,23)} = 0.6195$, $p = 0.6095$; ESC, $F_{(3,23)} = 0.6724$, $p = 0.5777$; FST: FLX, $F_{(1,30)} = 0.0358$, $p = 0.8512$; ESC, $F_{(1,27)} = 1.458$, $p = 0.2377$. Data are mean ± SE. *$p < 0.05$; **$p < 0.01$; ***$p < 0.001$ for drug versus VEH, or as indicated, by two-way ANOVA, Tukey's post-test. No differences between genotypes were observed in control measures for NSF (latency to feed, food consumption), EPM (closed arm time), or in the LD test (see Figure 3-1, available at https://doi.org/10.1523/JNEUROSCI.0352-18.2018.f3-1).

as PFC or hippocampus (Fig. 1-1, available at https://doi.org/10.1523/JNEUROSCI.0352-18.2018.f1-1). In *1AcKO* versus *WT* mice, there was a 90% reduction in 5-HT1A-stained TPH^+ cells in the dorsal raphe (Fig. 1*C*,*E*), indicating a strong reduction in 5-HT1A autoreceptors. This reduction in 5-HT1A receptors was confirmed using [^{125}I]-MPPI to detect specific 5-HT1A receptor binding. In the raphe nuclei, a ~60% reduction in specific binding was detected (Fig. 2*A*, *C*), whereas no change was seen in the hippocampus (Fig. 2*B*, *D*).

The function of 5-HT1A autoreceptors *in vivo* was addressed by measuring DPAT-induced hypothermia because in mice this response is dependent on 5-HT1A autoreceptors (Richardson-Jones et al., 2011). In contrast to *WT* littermates, in both male and female *1AcKO* mice, the DPAT-induced hypothermia response was abolished (Figs. 2*E*, Fig. 2-1, available at https://doi.org/10.1523/JNEUROSCI.0352-18.2018.f2-1, Fig. 2-2, available at https://doi.org/10.1523/JNEUROSCI.0352-18.2018.f2-2). We next assessed the function of 5-HT1A autoreceptors by whole-cell electrophysiological recordings of dorsal raphe 5-HT neurons in acute midbrain slices (Fig. 2*F*). Bath administration of the nonselective 5-HT1A agonist 5-CT induced a robust outward current that was evident in every recording from 5-HT neurons in *WT* slices. In contrast, the magnitude of this current was much reduced in recordings from *1AcKO* 5-HT cells, being noticeable in only one recording. Together, these results outline the effective abolishment of functional 5-HT1A autoreceptors in 5-HT neurons from *1AcKO* mice.

Anxiogenic actions of subchronic SSRI treatment in *1AcKO* mice

Next, we addressed the behavioral phenotype of the *1AcKO* mice. Because preliminary studies had shown no difference in baseline anxiety and depression behavior between *WT* and *1AcKO* mice in males and females (Luckhart, 2015), we pooled data from both sexes shown as blue and pink symbols, respectively. Previously, mice with a 30% suppression of 5-HT1A autoreceptors showed a

←

(*Figure legend continued.*) F-SalWT, 38.1 ± 0.32; KO, 38.2 ± 0.47; F-DPAT WT, 38.2 ± 0.27; KO, 38.2 ± 0.31. ***F***, Reduced 5-HT1A-mediated outward currents in *1AcKO* mice. Whole-cell voltage-clamp recordings of DR 5-HT neurons from *WT* (*n* = 6) and *1AcKO* (KO, *n* = 7) mice. Left, Time course of 5-HT1A-mediated outward current in response to 5-CT (100 nM; $V_m = -55$ mV). Right, Average peak steady-state 5-HT1AR-mediated currents from recorded 5-HT neurons. Data are mean ± SE. *$p < 0.05$ (unpaired two-tailed Student's *t* test).

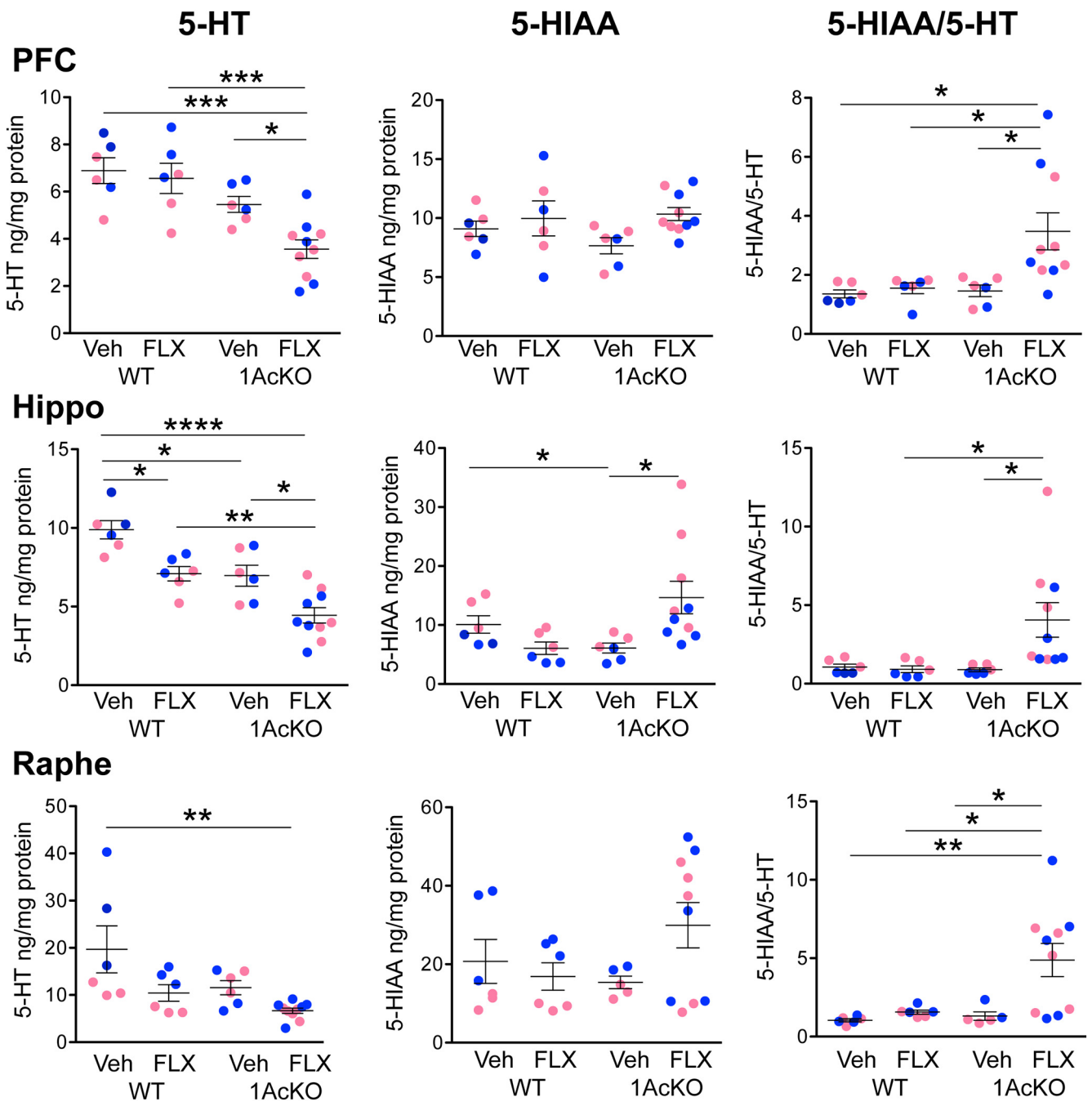

Figure 4. Enhanced 5-hydroxy indole acetic acid (5-HIAA)/5-HT in FLX-treated *1AcKO* mice. Tissue 5-HT and 5-HIAA content in WT and *1AcKO* mice was quantified in prefrontal cortex (PFC), hippocampus (Hippo), and dorsal raphe (DR) following fluoxetine (FLX) or vehicle (Veh) treatment (21–23 d), and the 5-HIAA/5-HT ratio calculated. Data points from individual male (M, blue) and female (F, pink) mice are shown. FLX treatment increased 5-HIAA/5-HT ratio in all 1AcKO tissues, and a significant reduction in 5-HT and increase in 5-HIAA was seen in FLX-treated *1AcKO* PFC and hippocampus, whereas only partial or no effects were seen in WT. For WT (Veh, FLX), n (M/F) = 3/3, 3/3; for KO, n = 3/3, 5/5. Data are mean ± SE. *$p < 0.05$ (two-way ANOVA, Tukey's post-test). **$p < 0.01$ (two-way ANOVA, Tukey's post-test). ***$p < 0.001$ (two-way ANOVA, Tukey'spost-test). ****$p < 0.0001$ (two-way ANOVA, Tukey'spost-test). For treatment × genotype interaction, see Figure 4-1 (available at https://doi.org/10.1523/JNEUROSCI.0352-18.2018.f4-1).

more rapid and robust FLX-induced reduction in anxiety in the NSF test (Richardson-Jones et al., 2010). Hence, we examined whether subchronic treatment with SSRIs affected behavior in the *1AcKO*, with a 90% reduction in 5-HT1A autoreceptors. As a first step, we investigated the effects of two SSRI treatments in the NSF anxiety test. Whereas subchronic FLX or ESC treatment had no effect in WT mice, we observed a significant increase in latency to feed in novel cage in *1AcKO*, indicative of increased anxiety (Fig. 3*A*,*B*). As controls for hunger/motivation, we found no difference in latency to feed or food consumption in the home cage (Fig. 3-1*A*, available at https://doi.org/10.1523/JNEUROSCI.0352-18.2018.f3-1). To further establish the development of an anxiogenic effect of SSRI treatment in the *1AcKO*, these mice were subjected to the LD and EPM tests. In the LD test (Fig. 3-1*B*, available at https://doi.org/10.1523/JNEUROSCI.0352-18.2018.f3-1), we failed to see any difference between the groups of mice in time or latency to enter the light side, suggesting no effect in this mild anxiety test. In the EPM, FLX induced a significant reduction in

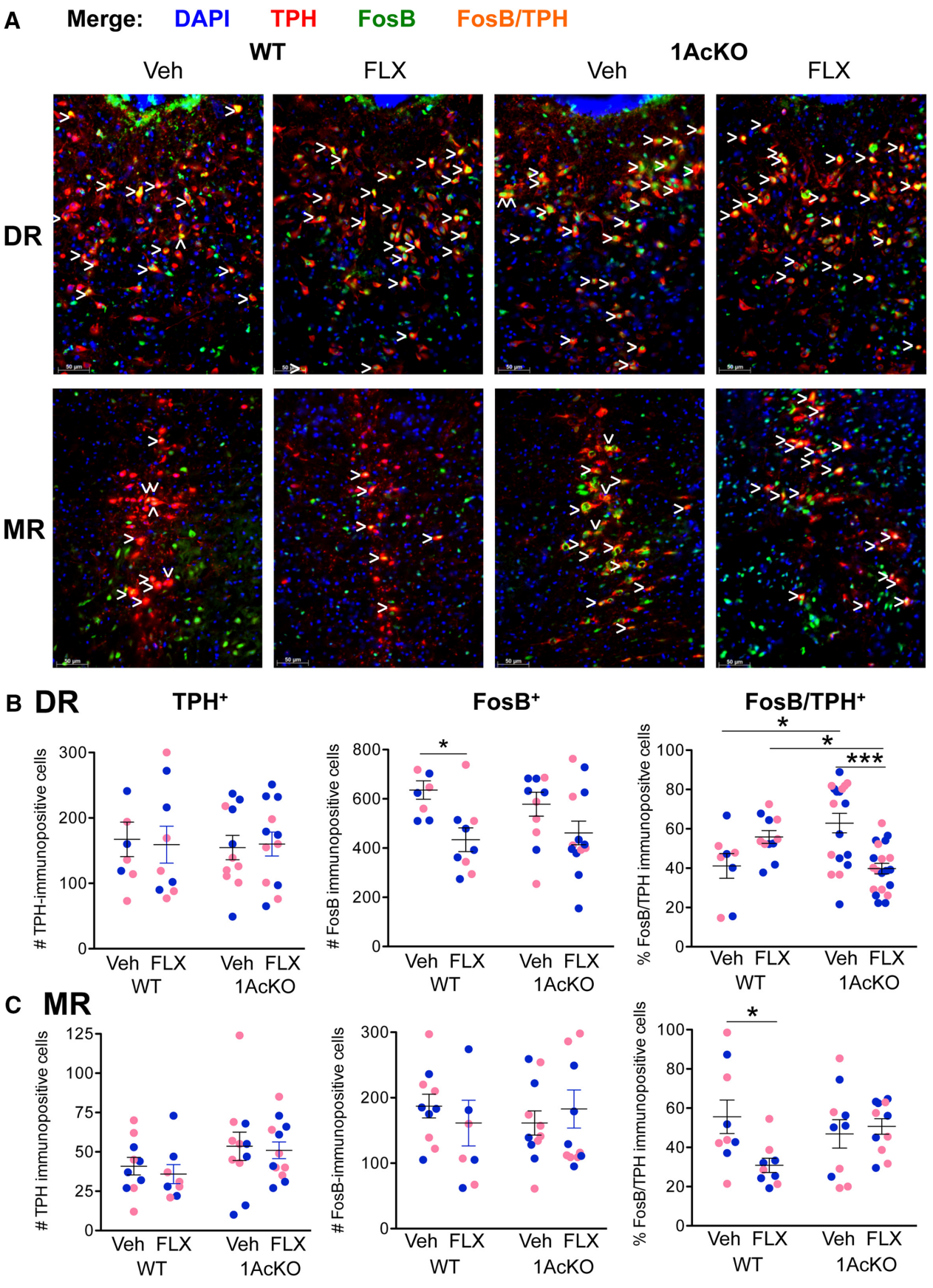

Figure 5. Opposite fluoxetine (FLX)-induced FosB changes in 5-HT neurons of *1AcKO* versus *WT* mice. Vehicle (Veh) or FLX was administered to WT and *1AcKO* mice for 24 d. ***A***, Merge of immunofluorescence staining of dorsal (DR) and median (MR) raphe nuclei using DAPI (nuclei), anti-TPH (5-HT marker), and anti-FosB (chronic activity marker) from *WT* (left) or *1AcKO* (right) mice. Carat symbols represent examples of FosB/TPH $^{+}$ cells. For images of single staining, see Figure 5-2 (available at https://doi.org/10.1523/JNEUROSCI.0352-18.2018.f5-2). ***B***, ***C***, Quantification of total TPH $^{+}$, FosB $^{+}$, and FosB/TPH $^{+}$ cells in dorsal (***B***) and median (***C***) raphe for male (M, blue) and female (F, pink) mice. In dorsal raphe, FLX reduced TPH/FosB $^{+}$ cells in *1AcKO* (*Figure legend continues.*)

open arm time in *1AcKO* but not *WT*, whereas ESC had no significant effect. No effect was seen on closed arm time or on total distance traveled in the maze (Fig. 3-1*C*, available at https://doi.org/10.1523/JNEUROSCI.0352-18.2018.f3-1). The effect of FLX on depression-related behavior was addressed by measuring the immobility time in the TS and FST (Fig. 3*C*,*D*). In both tests, FLX had no effect on the immobility time in *WT* or *1AcKO* mice. These data indicate that subchronic treatment with SSRIs is anxiogenic in *1AcKO* mice.

FLX-induced 5-HT metabolism and cellular activity in *1AcKO* mice

Because 5-HT1A autoreceptors negatively regulate 5-HT neuronal activity, we hypothesized that *1AcKO* mice treated with FLX may show increased release of 5-HT, resulting in increased levels of the metabolite, 5-HIAA. To test this, we measured both 5-HT and 5-HIAA levels in PFC, hippocampus, and raphe tissues (Fig. 4; statistics, Fig. 4-1, available at https://doi.org/10.1523/JNEUROSCI.0352-18.2018.4-1). There was a significant decrease in basal 5-HT and 5-HIAA levels only in the hippocampus of vehicle-treated *1AcKO* compared with *WT* mice. In hippocampus, FLX treatment reduced 5-HT levels in both *WT* and *1AcKO* but increased 5-HIAA only in the *1AcKO*, resulting in increased 5-HIAA/5-HT ratio. In all tissues, subchronic FLX treatment reduced 5-HT levels more strongly in *1AcKO* than in *WT* mice. This led to a significant increase in 5-HIAA/5-HT ratio in all tissues of *1AcKO* mice with no change in *WT* mice. Thus, loss of 5-HT1A autoreceptors results in increased 5-HT metabolism in PFC, hippocampus, and raphe in response to subchronic FLX treatment.

We next addressed whether neuronal activity of the raphe or other brain regions was altered in *1AcKO* mice treated with FLX (Fig. 3, timeline), using FosB staining after death as a marker for chronic neuronal activation (Figs. 5, 6). In the raphe, there were no changes in the number of 5-HT neurons (TPH^+ cells, Fig. 5*B*,*C*; statistics, Fig. 5-1, available at https://doi.org/10.1523/JNEUROSCI.0352-18.2018.f5-1, Fig. 5-2, available at https://doi.org/10.1523/JNEUROSCI.0352-18.2018.f5-2). However, the number of $FosB/TPH^+$ neurons was increased in *1AcKO* dorsal raphe, suggesting a higher level of chronic neuronal activation (Fig. 5*B*). In *1AcKO* mice, treatment with FLX induced a reduction in $FosB/TPH^+$ dorsal raphe cells, but had no effect in *WT*. Oppositely in the median raphe (Fig. 5*C*), FLX reduced $FosB/TPH^+$ cells in *WT*, but no change was seen in *1AcKO* sections. Thus, dorsal and median raphe showed differential regulation upon depletion of 5-HT1A autoreceptors and chronic treatment with FLX.

$FosB^+$ cells were found in several brain regions and were quantified to correlate with FLX-induced anxiety (Figs. 6, Fig. 6-1, available at https://doi.org/10.1523/JNEUROSCI.0352-18.2018.f6-1). Comparing vehicle-treated *1AcKO* with *WT*, significant reductions in $FosB^+$ cells were seen in EC, CA2/3, MSN, and Amy, and an increase in NAc. FLX treatment reduced $FosB^+$ cell counts in several regions of *WT* but not *1AcKO* mice (CA1, DG, MSN), and more strongly in EC of *WT* compared with *1AcKO* mice. FLX-treated *1AcKO* showed the most robust reductions in FosB in CA1, DG, Amy, and LHb, compared with *WT*. Thus, there was a reduced effect of FLX treatment in several brain regions in *1AcKO* compared with *WT*, but regions in which FLX response was more robust in *1AcKO* mice may contribute to the altered behavioral response.

Discussion

Role of reduced 5-HT1A autoreceptors in SSRI-induced anxiety

In this study, we have generated the *1AcKO* mice with 5-HT neuron-specific KO of the *HTR1A* gene to probe the role of 5-HT1A autoreceptors in behavior and response to subchronic SSRI treatment. Previously, early life suppression of 5-HT1A autoreceptor expression was shown to induce a developmental anxiety phenotype in the LD and open field tests that was not seen upon 5-HT1A autoreceptor suppression in adulthood (Richardson-Jones et al., 2010, 2011). To avoid developmental effects, we addressed whether inducible KO of the 5-HT1A autoreceptor in adulthood would affect behavior. We found that the *1AcKO* have a 90% reduction in 5-HT1A receptor-positive 5-HT neurons, although total binding of 5-HT1A autoreceptors in the raphe was reduced by only ~60%. This may reflect background from 5-HT1A receptors in nonserotonergic neurons (Fig. 1*C*), such as GABAergic interneurons (Bonnavion et al., 2010). Using electrophysiology, we found that 5-HT1A-mediated currents in 5-HT neurons were largely absent in *1AcKO* slices. Similarly, DPAT-induced hypothermia was abolished in *1AcKO* mice (Fig. 2*E*), indicating impaired 5-HT1A autoreceptor function *in vivo*.

In the *1AcKO* mice, baseline (or vehicle) anxiety and depression behaviors did not differ from the *WT* littermates in the tests used, consistent with our findings in *1AcKO* mice on a different genetic background with 80% loss of binding (Vahid-Ansari et al., 2017), and with findings following adulthood suppression of 5-HT1A autoreceptors by 30% (Richardson-Jones et al., 2010). However, transient siRNA-mediated suppression of 5-HT1A autoreceptors by 30%–40% for up to 3 d in C57BL/6 mice resulted in an antidepressed effect in the TS and FST, with no change in anxiety in the EPM test (Bortolozzi et al., 2012). In our studies, depletion of 5-HT1A autoreceptors was more extensive and chronic (FST and TS were done >32 d after tamoxifen). In this time, compensatory mechanisms, such as recurrent inhibition from prefrontal cortical projections to raphe GABAergic neurons (Geddes et al., 2016), may have normalized behavior. Conversely, increasing 5-HT1A autoreceptor levels by 50% in adulthood upon deletion of the repressor Freud-1/CC2D1A in 5-HT neurons results in anxiety and depression phenotypes that are resistant to chronic FLX treatment (Vahid-Ansari et al., 2017). Sex-dependent anxiety and depression phenotypes have been reported in other mouse models with similar upregulation of 5-HT1A autoreceptors (Luckhart et al., 2016; Philippe et al., 2018). Although we tested both sexes here, our ability to detect sex differences was underpowered. In contrast, transgenic overexpression of adult 5-HT1A autoreceptors by several-fold results in an aggression phenotype (Audero et al., 2013). However, our results suggest that deletion of adult 5-HT1A autoreceptors does not alter baseline anxiety/depression-like behaviors, although we did not test for effects on stress resiliency. The lack of behavioral response to subchronic FLX in the *WT* mice may indicate their insensitivity to the antidepressant effects of enhancing serotonin.

The anxiogenic response to subchronic SSRI treatment of *1AcKO* mice was unexpected. In previous studies, a striking an-

←

(*Figure legend continued.*) but not *WT*; in median raphe, FLX reduced $TPH/FosB^+$ cells in *WT* but not *1AcKO*. For DR (TPH^+, $FosB^+$, $TPH/FosB^+$), *n* (M/F (outliers)) = 3/4, 3/4, 4/4 (WT-Veh); 4/5, 5/4, 6/5 (WT-FLX); 5/6, 5/5, 8/8 (1) (KO-Veh); 7/5, 8/5, 11/9 (1) (KO-FLX); for MR, *n* = 5/5, 5/5, 5/5 (1) (WT-Veh); 4/4, 3/3, 4/5 (WT-FLX); 5/6, 5/6, 5/5 (1) (KO-Veh); 6/6, 5/6, 6/5 (1) (KO-FLX). Significant treatment × genotype interaction was detected for $FosB/TPH^+$ cells in both DR and MR (Figure 5-1, available at https://doi.org/10.1523/JNEUROSCI.0352-18.2018.f5-1). Data are mean ± SE. $^*p < 0.05$ (two-way ANOVA, Tukey's post-test). $^{***}p < 0.001$ (two-way ANOVA, Tukey's post-test).

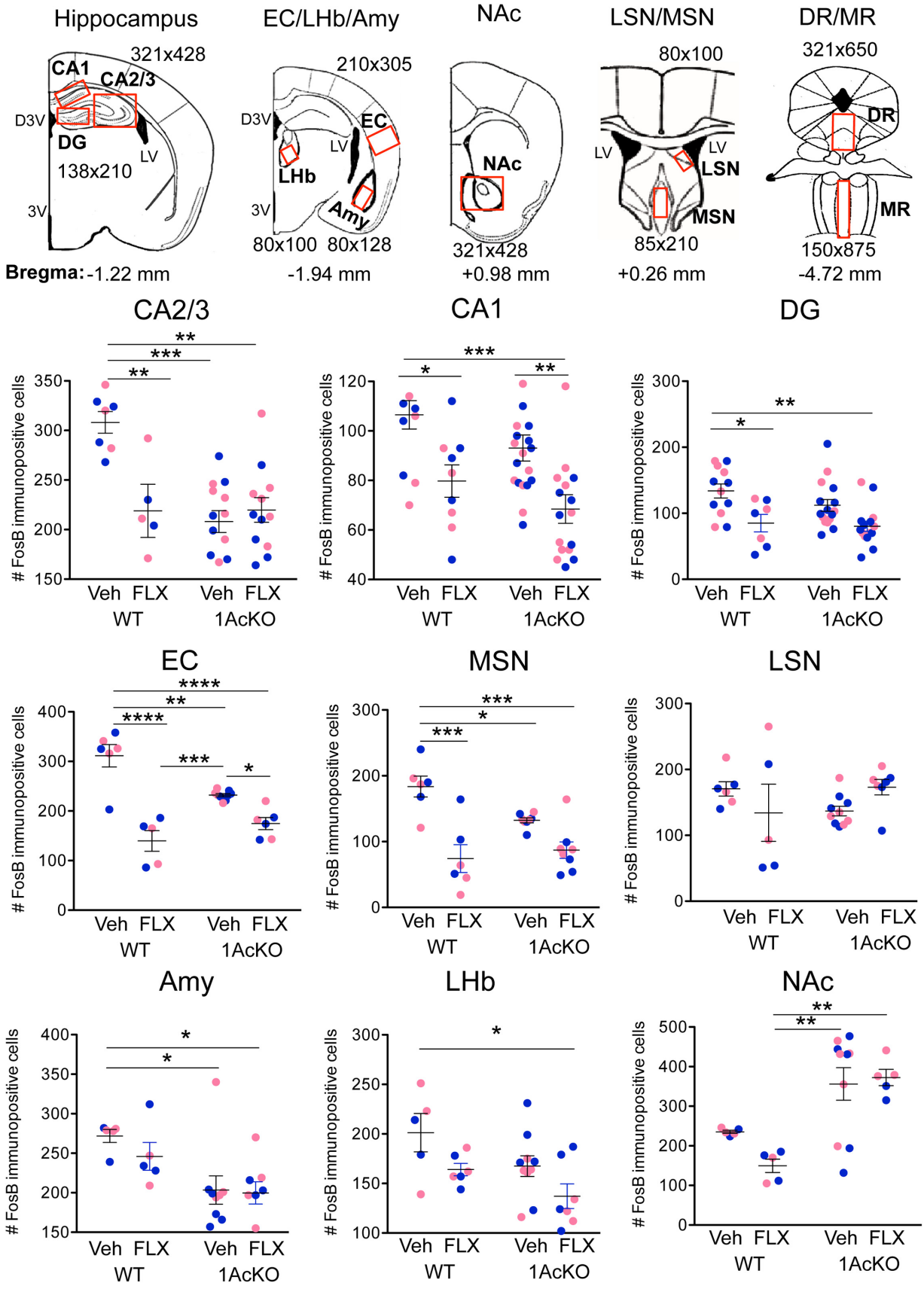

Figure 6. Brain regional differences in FLX-induced FosB changes in *1AcKO* versus *WT* mice. Shown above are figurative images of coronal sections at bregma levels (Paxinos and Franklin, 2001) and including regions of interest and templates ($\mu m \times \mu m$) used for cell counting. Vehicle (Veh) or FLX was administered to mice for 24 d. Immunofluorescence staining for FosB was compared in *1AcKO* and *WT* brain sections showing detectable FosB, and FosB$^+$ cells were quantified and plotted for male (M, blue) and female (F, pink) mice. For WT-Veh, FLX and KO-Veh, FLX, *n* (M/F (outliers)): hippocampal CA2/3 (4/3, 3/2, 6/6 (1), 6/6 (2)), CA1 (4/4, 4/4, 11/8 (2), 7/8), DG (6/6, 4/3, 9/7 (1), 9/6 (2)); EC (3/3, 3/2, 4/3 (2), 3/3 (2)); MSN (3/3, 3/3, (*Figure legend continues.*)

xiolytic effect of subchronic FLX treatment was seen in the NSF test in mice with a 30% suppression of 5-HT1A autoreceptors, but not in normal mice (Richardson-Jones et al., 2010) similar to our *WT* mice. The main difference is the more extensive reduction in 5-HT1A autoreceptors in our *1AcKO* mice. Upon SSRI treatment of *1AcKO* mice, serotonin-induced inhibition of 5-HT1A-positive GABAergic raphe neurons (Bonnavion et al., 2010) could further reduce local inhibition of 5-HT neurons, in addition to loss of 5-HT1A autoreceptors. This synergistic effect upon SSRI-induced blockade of reuptake could drive the anxiogenic response. A likely candidate for this effect is the ratio of median to dorsal raphe activity, which has been shown to correlate with anxiety in the postnatal FLX model of anxiety-depression (Teissier et al., 2015). The *1AcKO* mice appeared resistant to median raphe inactivation upon chronic SSRI treatment but displayed reduced activity of 5-HT neurons in the dorsal raphe (Fig. 5*C*).

Alterations in basal and FLX-induced brain networks upon loss of 5-HT1A autoreceptors

Although we did not detect baseline behavioral changes in *1AcKO* mice in the assays used, loss of 5-HT1A autoreceptors did have functional effects on responses to acute DPAT (reduced hypothermia), subchronic FLX (increased 5-HT metabolism and anxiety), and on basal and FLX-induced neuronal activity. Following subchronic (11 d) FLX treatment at a clinically relevant dose that partially blocks 5-HT reuptake (Vahid-Ansari et al., 2017), the 5-HIAA/5-HT ratio was increased in *1AcKO* PFC, hippocampus, and raphe compared with *WT*. This increase in 5-HT metabolism is consistent with increased FLX-induced 5-HT release that could result from increased firing of 5-HT neurons upon loss of 5-HT1A autoreceptors in the *1AcKO* mice. Similarly, 8 d subchronic, but not chronic, FLX treatment induced >2-fold increase in 5-HT release in hippocampus but not PFC of mice with adult suppression of 5-HT1A autoreceptors (Richardson-Jones et al., 2010). The lack of change in basal 5-HT or 5-HIAA in raphe and PFC is consistent with the lack of behavioral phenotype in untreated or vehicle-treated *1AcKO* compared with *WT* mice.

Interestingly, FosB activity in dorsal and median raphe was differentially altered: FLX inhibited dorsal raphe FosB but maintained FosB in median raphe (Fig. 5*B*). The median raphe projects mainly to the septum and hippocampus, whereas the rostral dorsal raphe projects to amygdala, NAc, and PFC (Commons, 2016; Muzerelle et al., 2016). In rats, microinjection of 5-HT1A antagonist WAY100635 or neuronal activator kainate in the median raphe is anxiogenic, and this effect was blocked by intrahippocampal injection of WAY100635, implicating a median raphe-dorsal hippocampal circuit in anxiety (Dos Santos et al., 2008). Optogenetic or chemogenetic activation of median raphe 5-HT neurons in mice elicits anxiety-like behavior (Ohmura et al., 2014; Teissier et al., 2015). These results suggest that maintained FLX-induced 5-HT release from median raphe-hippocampal projections (Muzerelle et al., 2016) may mediate increased anxiety-like behavior in the *1AcKO* mice (Belzung et al., 2014). On the other hand, optogenetic stimulation of hippocampal DG granule cells has a rapid antianxiety effect (Kheirbek et al., 2013), and 5-HT1A heteroreceptors on these cells are required for the antianxiety effect of chronic FLX treatment in the NSF (Samuels et al., 2015). Hence, different populations of hippocampal neurons may mediate the proanxiety and antianxiety of actions of FLX treatment.

Comparing *1AcKO* with *WT* mice, basal FosB activity was altered in three brain areas that are linked via the fimbria-fornix pathway, with reduced FosB in EC, CA2/3, and MSN. This pathway is important for spatial information processing; however, because the assays we used did not specifically test for this, we did not see any difference between *1AcKO* and *WT* behaviors. However, in *1AcKO* versus *WT* mice, a reduced FLX-induced inhibition of FosB was seen in these regions and additional hippocampal and medial septal areas, suggesting a more widespread and robust effect. The septohippocampal pathway is implicated in sensory gating of spatial information (Kaifosh et al., 2013) and is innervated by the median raphe (Szonyi et al., 2016). Maintenance of median raphe activity to enhance 5-HT release in these areas after FLX in the *1AcKO* mice may have contributed to the anxiety phenotype (Dos Santos et al., 2008; An et al., 2016). Interestingly, both NSF and EPM rely on spatial cues to elicit anxiety more than the LD box test, which may more robustly recruit hippocampal input.

We have previously seen that multiple brain regions are activated in a mouse model of poststroke anxiety and depression (Vahid-Ansari and Albert, 2018). Importantly, chronic FLX treatment reversed the anxiety and depression phenotypes in this poststroke model, and reduced FosB in glutamatergic cells in most brain regions, including PFC, hippocampus, and lateral septum. By contrast, the inability of FLX to reduce FosB in the *1AcKO* compared with *WT* mice was associated with its anxiogenic effect. This suggests that the combination of genotype and FLX treatment results in hyperactivation of the 5-HT system that could contribute to FLX-induced anxiety in the *1AcKO* mice, but is not the only factor.

Clinical relevance of low 5-HT1A autoreceptors

These findings may have implications for SSRI-induced anxiogenic responses seen clinically following subchronic treatment, particularly in adolescence (Sinclair et al., 2009; Goldsmith and Moncrieff, 2011; Olivier et al., 2011). Comparing transgenic/KO mouse models that alter 5-HT neurotransmission, a U-shaped relation to anxiety is seen: increased anxiety occurs in models with very low 5-HT, as well as models with elevated 5-HT release (Albert et al., 2014). Depression-like behavior is associated with reduced 5-HT in mouse models (Albert et al., 2014). Our data suggest that hyperactivation of 5-HT release in *1AcKO* mice treated with subchronic FLX increases anxiety. Because 5-HT1A autoreceptors are expressed at low levels in mice until late adolescence (p21–p30) (Richardson-Jones et al., 2011), the reduced binding in *1AcKO* mice mimics this aspect of adolescent 5-HT regulation. Transient suppression of 5-HT1A autoreceptors by 40% during this period of adolescence (p14–30) induces baseline anxiety-like behavior in mice (Donaldson et al., 2014). Similarly, chronic FLX treatment in adolescence increases anxiety-like behavior in mice (Oh et al., 2009; Iñiguez et al., 2014) and is associated with risk of suicide in human youths (Olivier et al., 2011). The region-specific activity changes that associate with anxiety in the *1AcKO* mice may provide insight into aberrant clinical responses to SSRI treatment.

In conclusion, upon KO of 5-HT1A autoreceptors in adulthood, we did not find changes in anxiety- or depression-like

←

(*Figure legend continued.*) 4/4 (2), 4/4); LSN (3/3, 3/3, 5/5, 4/3); Amy (2/3 (1), 2/1 (2), 5/4 (1), 3/4); LHb (3/2 (1), 2/2 (1), 5/5 (1), 4/3 (1)); NAc (2/3, 2/3, 5/4 (1), 2/3 (2)). Significant treatment × genotype interaction was detected for EC, CA2/3, MSN, with trend for LSN (Figure 6-1, available at https://doi.org/10.1523/JNEUROSCI.0352-18.2018.f6-1). Data are mean ± SE. Two-way ANOVA, Tukey's post-test: $*p < 0.05$; $**p < 0.01$; $***p < 0.001$; $****p < 0.0001$.

behaviors in *1AcKO* mice. However, we did find increased activity of 5-HT neurons, and a paradoxical anxiogenic response to subchronic FLX treatment that may be driven by increased median raphe 5-HT release and activation of septohippocampal pathways.

References

aan het Rot M, Mathew SJ, Charney DS (2009) Neurobiological mechanisms in major depressive disorder. CMAJ 180:305–313. CrossRef Medline

Albert PR (2012) Transcriptional regulation of the 5-HT1A receptor: implications for mental illness. Philos Trans R Soc Lond B Biol Sci 367:2402–2415. CrossRef Medline

Albert PR, Lemonde S (2004) 5-HT1A receptors, gene repression, and depression: guilt by association. Neuroscientist 10:575–593. CrossRef Medline

Albert PR, Lembo P, Storring JM, Charest A, Saucier C (1996) The 5-HT1A receptor: signaling, desensitization, and gene transcription. Neuropsychopharmacology 14:19–25. CrossRef Medline

Albert PR, Vahid-Ansari F, Luckhart C (2014) Serotonin-prefrontal cortical circuitry in anxiety and depression phenotypes: pivotal role of pre- and post-synaptic 5-HT1A receptor expression. Front Behav Neurosci 8:199. CrossRef Medline

An Y, Chen C, Inoue T, Nakagawa S, Kitaichi Y, Wang C, Izumi T, Kusumi I (2016) Mirtazapine exerts an anxiolytic-like effect through activation of the median raphe nucleus-dorsal hippocampal 5-HT pathway in contextual fear conditioning in rats. Prog Neuropsychopharmacol Biol Psychiatry 70:17–23. CrossRef Medline

Audero E, Mlinar B, Baccini G, Skachokova ZK, Corradetti R, Gross C (2013) Suppression of serotonin neuron firing increases aggression in mice. J Neurosci 33:8678–8688. CrossRef Medline

Belzung C, Turiault M, Griebel G (2014) Optogenetics to study the circuits of fear- and depression-like behaviors: a critical analysis. Pharmacol Biochem Behav 122:144–157. CrossRef Medline

Berger SM, Weber T, Perreau-Lenz S, Vogt MA, Gartside SE, Maser-Gluth C, Lanfumey L, Gass P, Spanagel R, Bartsch D (2012) A functional Tph2 C1473G polymorphism causes an anxiety phenotype via compensatory changes in the serotonergic system. Neuropsychopharmacology 37:1986–1998. CrossRef Medline

Blier P, El Mansari M (2013) Serotonin and beyond: therapeutics for major depression. Philos Trans R Soc Lond B Biol Sci 368:20120536. CrossRef Medline

Boldrini M, Underwood MD, Mann JJ, Arango V (2008) Serotonin-1A autoreceptor binding in the dorsal raphe nucleus of depressed suicides. J Psychiatr Res 42:433–442. CrossRef Medline

Bonnavion P, Bernard JF, Hamon M, Adrien J, Fabre V (2010) Heterogeneous distribution of the serotonin 5-HT(1A) receptor mRNA in chemically identified neurons of the mouse rostral brainstem: implications for the role of serotonin in the regulation of wakefulness and REM sleep. J Comp Neurol 518:2744–2770. CrossRef Medline

Bortolozzi A, Castañé A, Semakova J, Santana N, Alvarado G, Cortés R, Ferrés-Coy A, Fernández G, Carmona MC, Toth M, Perales JC, Montefeltro A, Artigas F (2012) Selective siRNA-mediated suppression of 5-HT1A autoreceptors evokes strong anti-depressant-like effects. Mol Psychiatry 17:612–623. CrossRef Medline

Calizo LH, Akanwa A, Ma X, Pan YZ, Lemos JC, Craige C, Heemstra LA, Beck SG (2011) Raphe serotonin neurons are not homogenous: electrophysiological, morphological and neurochemical evidence. Neuropharmacology 61:524–543. CrossRef Medline

Cipriani A, Furukawa TA, Salanti G, Geddes JR, Higgins JP, Churchill R, Watanabe N, Nakagawa A, Omori IM, McGuire H, Tansella M, Barbui C (2009) Comparative efficacy and acceptability of 12 new-generation antidepressants: a multiple-treatments meta-analysis. Lancet 373:746–758. CrossRef Medline

Commons KG (2016) Ascending serotonin neuron diversity under two umbrellas. Brain Struct Funct 221:3347–3360. CrossRef Medline

Coplan JD, Gopinath S, Abdallah CG, Berry BR (2014) A neurobiological hypothesis of treatment-resistant depression: mechanisms for selective serotonin reuptake inhibitor non-efficacy. Front Behav Neurosci 8:189. CrossRef Medline

Czesak M, Le François B, Millar AM, Deria M, Daigle M, Visvader JE, Anisman H, Albert PR (2012) Increased serotonin-1A (5-HT1A) autoreceptor expression and reduced raphe serotonin levels in deformed epidermal autoregulatory factor-1 (Deaf-1) gene knock-out mice. J Biol Chem 287:6615–6627. CrossRef Medline

Donaldson ZR, Piel DA, Santos TL, Richardson-Jones J, Leonardo ED, Beck SG, Champagne FA, Hen R (2014) Developmental effects of serotonin 1A autoreceptors on anxiety and social behavior. Neuropsychopharmacology 39:291–302. CrossRef Medline

Dos Santos L, de Andrade TG, Zangrossi Junior H (2008) 5-HT1A receptors in the dorsal hippocampus mediate the anxiogenic effect induced by the stimulation of 5-HT neurons in the median raphe nucleus. Eur Neuropsychopharmacol 18:286–294. CrossRef Medline

Garcia-Garcia AL, Newman-Tancredi A, Leonardo ED (2014) 5-HT(1A) receptors in mood and anxiety: recent insights into autoreceptor versus heteroreceptor function. Psychopharmacology (Berl) 231:623–636. CrossRef Medline

Geddes SD, Assadzada S, Lemelin D, Sokolovski A, Bergeron R, Haj-Dahmane S, Béïque JC (2016) Target-specific modulation of the descending prefrontal cortex inputs to the dorsal raphe nucleus by cannabinoids. Proc Natl Acad Sci U S A 113:5429–5434. CrossRef Medline

Goldsmith L, Moncrieff J (2011) The psychoactive effects of antidepressants and their association with suicidality. Curr Drug Saf 6:115–121. CrossRef Medline

Hesselgrave N, Parsey RV (2013) Imaging the serotonin 1A receptor using [11C]WAY100635 in healthy controls and major depression. Philos Trans R Soc Lond B Biol Sci 368:20120004. CrossRef Medline

Iñiguez SD, Alcantara LF, Warren BL, Riggs LM, Parise EM, Vialou V, Wright KN, Dayrit G, Nieto SJ, Wilkinson MB, Lobo MK, Neve RL, Nestler EJ, Bolaños-Guzman CA (2014) Fluoxetine exposure during adolescence alters responses to aversive stimuli in adulthood. J Neurosci 34:1007–1021. CrossRef Medline

Jans LA, Riedel WJ, Markus CR, Blokland A (2007) Serotonergic vulnerability and depression: assumptions, experimental evidence and implications. Mol Psychiatry 12:522–543. CrossRef Medline

Kaifosh P, Lovett-Barron M, Turi GF, Reardon TR, Losonczy A (2013) Septo-hippocampal GABAergic signaling across multiple modalities in awake mice. Nat Neurosci 16:1182–1184. CrossRef Medline

Kheirbek MA, Drew LJ, Burghardt NS, Costantini DO, Tannenholz L, Ahmari SE, Zeng H, Fenton AA, Hen R (2013) Differential control of learning and anxiety along the dorsoventral axis of the dentate gyrus. Neuron 77:955–968. CrossRef Medline

Krishnan V, Nestler EJ (2008) The molecular neurobiology of depression. Nature 455:894–902. CrossRef Medline

Luckhart C (2015) Functional studies of the 5-HT1A autoreceptor in mice. In: Neuroscience, p 128. Ottawa: University of Ottawa.

Luckhart C, Philippe TJ, Le François B, Vahid-Ansari F, Geddes SD, Béïque JC, Lagace DC, Daigle M, Albert PR (2016) Sex-dependent adaptive changes in serotonin-1A autoreceptor function and anxiety in Deaf1-deficient mice. Mol Brain 9:77. CrossRef Medline

McLean AC, Valenzuela N, Fai S, Bennett SA (2012) Performing vaginal lavage, crystal violet staining, and vaginal cytological evaluation for mouse estrous cycle staging identification. J Vis Exp 67:e4389. CrossRef Medline

Muzerelle A, Scotto-Lomassese S, Bernard JF, Soiza-Reilly M, Gaspar P (2016) Conditional anterograde tracing reveals distinct targeting of individual serotonin cell groups (B5–B9) to the forebrain and brainstem. Brain Struct Funct 221:535–561. CrossRef Medline

Northoff G (2013) Gene, brains, and environment-genetic neuroimaging of depression. Curr Opin Neurobiol 23:133–142. CrossRef Medline

Oh JE, Zupan B, Gross S, Toth M (2009) Paradoxical anxiogenic response of juvenile mice to fluoxetine. Neuropsychopharmacology 34:2197–2207. CrossRef Medline

Ohmura Y, Tanaka KF, Tsunematsu T, Yamanaka A, Yoshioka M (2014) Optogenetic activation of serotonergic neurons enhances anxiety-like behaviour in mice. Int J Neuropsychopharmacol 17:1777–1783. CrossRef Medline

Olivier JD, Blom T, Arentsen T, Homberg JR (2011) The age-dependent effects of selective serotonin reuptake inhibitors in humans and rodents: a review. Prog Neuropsychopharmacol Biol Psychiatry 35:1400–1408. CrossRef Medline

Paxinos G, Franklin KB (2001) The mouse brain in stereotaxic coordinates, Ed 2. San Diego: Academic.

Philippe TJ, Vahid-Ansari F, Donaldson ZR, Le François B, Zahrai A, Turcotte-Cardin V, Daigle M, James J, Hen R, Merali Z, Albert PR (2018) Loss of MeCP2 in adult 5-HT neurons induces 5-HT1A autoreceptors, with opposite sex-dependent anxiety and depression phenotypes. Sci Rep 8:5788. CrossRef Medline

Piñeyro G, Blier P (1999) Autoregulation of serotonin neurons: role in antidepressant drug action. Pharmacol Rev 51:533–591. Medline

Richardson-Jones JW, Craige CP, Guiard BP, Stephen A, Metzger KL, Kung HF, Gardier AM, Dranovsky A, David DJ, Beck SG, Hen R, Leonardo ED (2010) 5-HT(1A) autoreceptor levels determine vulnerability to stress and response to antidepressants. Neuron 65:40–52. CrossRef Medline

Richardson-Jones JW, Craige CP, Nguyen TH, Kung HF, Gardier AM, Dranovsky A, David DJ, Guiard BP, Beck SG, Hen R, Leonardo ED (2011) Serotonin-1A autoreceptors are necessary and sufficient for the normal formation of circuits underlying innate anxiety. J Neurosci 31:6008–6018. CrossRef Medline

Rush AJ, Warden D, Wisniewski SR, Fava M, Trivedi MH, Gaynes BN, Nierenberg AA (2009) STAR*D: revising conventional wisdom. CNS Drugs 23:627–647. CrossRef Medline

Samuels BA, Anacker C, Hu A, Levinstein MR, Pickenhagen A, Tsetsenis T, Madroñal N, Donaldson ZR, Drew LJ, Dranovsky A, Gross CT, Tanaka KF, Hen R (2015) 5-HT1A receptors on mature dentate gyrus granule cells are critical for the antidepressant response. Nat Neurosci 18:1606–1616. CrossRef Medline

Santarelli L, Saxe M, Gross C, Surget A, Battaglia F, Dulawa S, Weisstaub N, Lee J, Duman R, Arancio O, Belzung C, Hen R (2003) Requirement of hippocampal neurogenesis for the behavioral effects of antidepressants. Science 301:805–809. CrossRef Medline

Sinclair LI, Christmas DM, Hood SD, Potokar JP, Robertson A, Isaac A, Srivastava S, Nutt DJ, Davies SJ (2009) Antidepressant-induced jitteriness/anxiety syndrome: systematic review. Br J Psychiatry 194:483–490. CrossRef Medline

Stockmeier CA, Shapiro LA, Dilley GE, Kolli TN, Friedman L, Rajkowska G (1998) Increase in serotonin-1A autoreceptors in the midbrain of suicide victims with major depression-postmortem evidence for decreased serotonin activity. J Neurosci 18:7394–7401. CrossRef Medline

Szonyi A, Mayer MI, Cserép C, Takács VT, Watanabe M, Freund TF, Nyiri G (2016) The ascending median raphe projections are mainly glutamatergic in the mouse forebrain. Brain Struct Funct 221:735–751. CrossRef Medline

Teissier A, Chemiakine A, Inbar B, Bagchi S, Ray RS, Palmiter RD, Dymecki SM, Moore H, Ansorge MS (2015) Activity of raphe serotonergic neurons controls emotional behaviors. Cell Rep 13:1965–1976. CrossRef Medline

Vahid-Ansari F, Albert PR (2018) Chronic fluoxetine induces activity changes in recovery from poststroke anxiety, depression, and cognitive impairment. Neurotherapeutics 15:200–215. CrossRef Medline

Vahid-Ansari F, Lagace DC, Albert PR (2016) Persistent post-stroke depression in mice following unilateral medial prefrontal cortical stroke. Transl Psychiatry 6:e863. CrossRef Medline

Vahid-Ansari F, Daigle M, Manzini MC, Tanaka KF, Hen R, Geddes SD, Béïque JC, James J, Merali Z, Albert PR (2017) Abrogated freud-1/Cc2d1a repression of 5-HT1A autoreceptors induces fluoxetine-resistant anxiety/depression-like behavior. J Neurosci 37:11967–11978. CrossRef Medline

Vialou V, Thibault M, Kaska S, Cooper S, Gajewski P, Eagle A, Mazei-Robison M, Nestler EJ, Robison AJ (2015) Differential induction of FosB isoforms throughout the brain by fluoxetine and chronic stress. Neuropharmacology 99:28–37. CrossRef Medline

Young SN, Leyton M (2002) The role of serotonin in human mood and social interaction. insight from altered tryptophan levels. Pharmacol Biochem Behav 71:857–865. CrossRef Medline